Proceedings of BioMed2007
2nd Frontiers in Biomedical Devices Conference
June 7-8, 2007, Irvine, California, USA

BIOMED2007-38006

DEVELOPMENT OF A TRACER FLUID IN A VERTICAL TUBE WITH GRAVITY-ASSISTED AND RESISTED MOTIONS

Chong Zhou and Joseph Majdalani[1]
Department of Mechanical, Aerospace and Biomedical Engineering
University of Tennessee (UTSI), Tullahoma, TN 37388-9700
drmajdalani@gmail.com

Christopher A. Dawson
Department of Physiology, Medical College of Wisconsin
Zablocki V. A. Medical Center, Milwaukee, WI 53295-1000

This study provides procedural tools that can be used in concert with a computer algorithm to simulate the two-phase flow development of a higher density, tracer fluid inside a vertical tube. The problem arises in the context of a tracer fluid (e.g., a contrast agent) being injected into a neutral fluid such as blood. Based on cell fractions of tracer fluid obtained numerically, absorbency profiles are extrapolated. These are shown to compare favorably with laboratory x-ray samples realized under similar flow conditions. At low Reynolds numbers, one finds that a downward profile exhibits a more elongated frontal boundary than predicted by laminar flow theory of a single-phase, Newtonian fluid. The observed stretching of the denser fluid is confirmed experimentally and can be attributed to the combined effects of gravity assistance near the core and viscous resistance near the wall. In gravity-resisted flow, a reverse behavior is observed. A blunter frontal boundary is established during upward motion. In both cases, the role of gravity is weakened with successive increases in the Reynolds number. This behavior suggests the existence of a Reynolds number above which gravitational bias can be neglected in any flow orientation. It is hoped that this study will set the pace for a broader investigation of two-phase motion characterization of a tracer fluid under various flow conditions and orientations.

1 INTRODUCTION

Use of radiopaque tracer fluid in x-ray angiographic measurement of spatial distribution of blood flow within an organ has been based on the assumption that the tracer fluid has the same properties as the blood except with regard to its x-ray absorbency. However, the greater x-ray absorbency is also associated with greater density. Thus, the extent to which the tracer fluid faithfully tracks the flow can depend on the flow conditions with respect to inertial, viscous and gravitational forces in this two-phase flow problem (see [1-4]). The physical model entails the two-phase development of a slug-shaped tracer fluid immersed in a primary fluid exhibiting a similar viscosity but a different density. Due to the disparity in tracer and primary fluid densities, the flow profile of the tracer fluid can become sensitive to gravitational bias [1-3]. The influence of gravity can, in turn, vary depending on the byproduct of flow orientation and inertia. In horizontal flow, asymmetry is expected with slow moving primary flows due to gravitational drag and subsequent sagging of the denser fluid. Conversely, the gravitational distortion is expected to become less appreciable in higher Reynolds number flows. In vertical flow, one expects the

[1] To whom correspondence should be addressed. Jack D. Whitfield Professor of High Speed Flows. Fellow ASME.

shape of the tracer fluid to be influenced by gravity depending on the flow direction. Clearly, characterization of the developing tracer fluid is an important step in determining the influence of a specific density difference between two fluids on the ability to faithfully track the flow [1-3].

The present study focuses on the development of a simulation technique intended for modeling the development of a slug-shaped tracer fluid that has been suddenly introduced into a primary, perfusion fluid. In the process, a numerical algorithm is described that allows for the extraction of data in a form directly comparable to those obtained using x-ray imaging [1-4]. This includes the reproduction of temporal and spatial absorbency profiles of the tracer fluid. In the present investigation, the simulation technique is applied to the vertical flow orientation in both upward and downward flow directions with comparisons between numerical simulations and experimental measurements. The prime objective of the study is to demonstrate the viability of a computer-based simulation technique in assessing the role of gravity on the shape of a tracer fluid having a density greater than the primary medium that guides the two-phase flow motion.

2 EXPERIMENTAL PROCEDURE

The intent of this simulation platform is to correspond as closely as practical to the experiment shown schematically in Fig. 1 [1]. The apparatus enables the introduction of a (secondary) tracer fluid (i.e., the contrast medium) into a pump-driven recirculation circuit filled with the primary fluid. The circuit includes a reservoir from which the primary fluid is pumped through an injection loop for introducing the contrast agent. The stream then passes through a vertical x-ray translucent tube that crosses the detection site of the x-ray beam before returning back to the reservoir. The tube has a 0.3175 cm inner diameter. The primary fluid is composed of 65% ethylene glycol and 35% water. Its density and viscosity are 1070 kgm^{-3} and 0.00587 $kgm^{-1}s^{-1}$, respectively. The tracer, on the other hand, is diatrizoate meglumine whose density and viscosity are 1250 kgm^{-3} and 0.00686 $kgm^{-1}s^{-1}$, respectively. The injector contains 25.3 cm of tracer fluid and is positioned at a distance of 31 cm upstream of the x-ray site. The effective length of tubing measured from the tube entrance to the x-ray site is 56.3 cm.

The injection loop includes a solenoid that is triggered to automatically block section 2 while opening section 3. This enables the tracer fluid to merge into the circuit as nearly a plug. In this experimental arrangement, the evolution of the tracer fluid under the action of gravity constitutes our main interest. Since the tracer has a density that exceeds that of the primary medium, its mass concentration can be detected at the x-ray site. To this end, an x-ray camera is used to record the absorbance at the rate of 30 frames per second. These photographs permit the extrapolation of experimental concentrations versus time data. A numerical simulation of the flow evolution in the entire tube is described next.

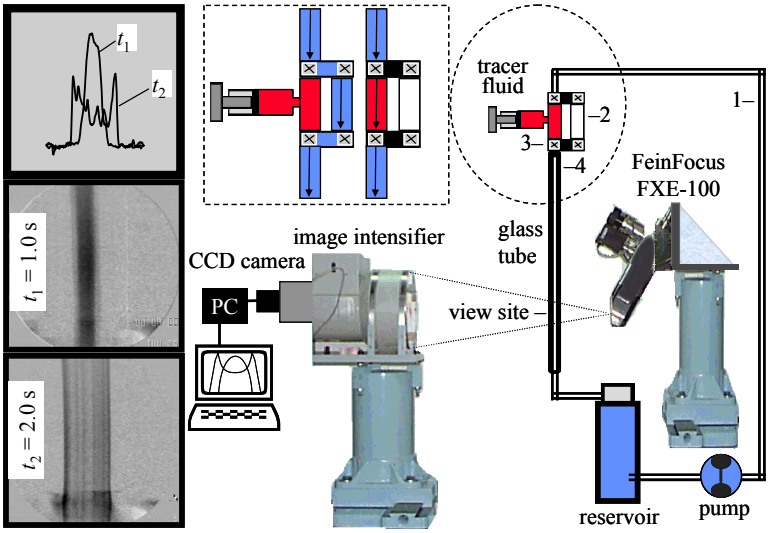

Fig. 1 Experimental setup.

3 COMPUTATIONAL MODEL

The first step in initiating the CFD simulation is to establish the geometric mesh. This is accomplished by first meshing one face at one end of the tube and then mapping that structure across the entire domain. The mesh used consists of an axisymmetric grid whose resolution follows a geometric progression in the radial direction (see Fig. 2a). Its increased density near the wall enables the resolution of rapid changes within the boundary layer. Conversely, its coarseness near the core helps reduce the overall computational effort.

To ensure that the computational domain is sufficiently long, the length of the tube is taken to be longer that the classic entrance length of a developing flow under laminar conditions. This length can be calculated from the approximate empirical relation $L_E / D = 0.06\,\mathrm{Re}$ [5]. In the numerical simulations, we choose $L/D \approx 178$, a value that permits the slug-shaped tracer fluid to exceed 99% of its fully-developed state before exiting the computational domain. To efficiently cover the elongated, slender domain, the cell aspect ratio in the longitudinal direction is chosen to be 8 at the core; it then increases with the geometric decrease in radial cell size as the wall is approached. Such a choice results in computational savings at no material loss in accuracy. In fact, a smaller aspect ratio does not lead to a noticeable change in the results. Throughout these simulations, a fixed mesh is used. A moving mesh that brackets the tracer fluid is not utilized because the evolving tracer can occupy the entire tube in its final developmental stages.

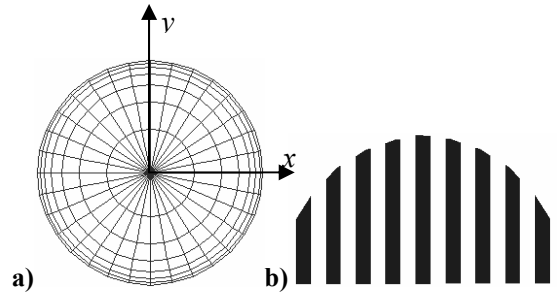

Fig. 2 Structure of a) the progressive mesh arrangement used in the simulations, and b) the subdivision of an isosurface (half shown) into finite strips parallel to the detection beam.

Velocity and continuative boundary conditions are imposed at the inlet and outlet sections of the tube. While a justifiably fully-developed flow of primary fluid is prescribed at the inlet, a continuative boundary condition for free outflow is allowed at the downstream end. In between inlet and outlet, the tube surface is modeled with symmetric wall boundary conditions that divide the domain in half about its midsection plane.

Having defined the geometric grid and its boundary conditions, the resulting mesh file is imported into a finite volume Navier-Stoke solver [6]. Flow options are then set to account for time-dependency and multiphase interactions. At this juncture, a user-defined link that reproduces the fully-developed Poiseuille flow at the inlet section of the tube is assigned to the primary fluid. The code is then initialized and executed. As a precautionary measure, a sensitivity analysis is carried out first. This is accomplished by repeating a given simulation using a doubly-meshed resolution. Once grid independence is affirmed, the program is applied to specific cases of interest. The finite volume solver used by the code employs multigrid acceleration. Multigrid acceleration reduces the error by iterating in an alternative fashion on a series of coarse and fine grids. The convergence criterion we have adopted is based on a tolerance that ensures that the residual error remains less than 10^{-3} in the momentum balance, and less than 10^{-7} in the energy balance.

4 RESULTS AND DISCUSSION

Insofar as gravitational corrections depend on flow attributes, they require full-scale investigations of the two-phase flow motion exhibited by the tracer fluid. Such investigations must take into consideration a wide arrary of flow conditions, density ratios, and flow orientations.

Four sample cases are used to simulate the laminar flow development of tracer fluid both experimentally and numerically. The four cases mimic two flow Reynolds numbers of 60 and 90 with both upward and downward flow motions. These values correspond to two pump rates of 50 and 75 ml/min, respectively. All experimental parameters used in the laboratory are later fed into the numerical code. Since the physical x-ray site is positioned at a distance of 31 cm downstream of the tracer fluid, an equivalent distance is used in the numerical code to record flow data.

Experimentally, the x-ray beam intersects the tube along a constant z–plane that we have called 'isosurface.' The intersection of this (x, y) plane with the image intensifier forms a unique detection line in the x–direction. By summing the above-background absorbency along the isosurface, one is able to measure the local fraction of tracer fluid as time elapses. Experimentally, we dynamically measure the line integral of the concentration of tracer fluid along the line of detection; this enables us to track its total fraction in the plane of detection with the passage of time. While x-ray imagery can be easily converted into concentration curves at the site of detection, post-processing of numerical simulations is needed to provide comparable sampling.

To extract similar results from the numerical code, an isosurface is divided into several strips perpendicular to the x–axis. In Fig. 2b, 9 different strips (i.e., bins) are chosen to cover the semi-circular cross section. Due to symmetry, half of the domain is considered only. Since the CFD output includes volume fractions of primary and secondary fluids at each cell, integrating the volume fraction of secondary fluid along each strip permits the measurement of equivalent x-ray absorbance detected by a virtual beam crossing that strip longitudinally (i.e., in the y–direction). This numerically calculated value is directly proportional to the absorbency level at that particular point. By measuring the fraction of tracer fluid along the line of detection, we are able to predict the absorbency (i.e., concentration of secondary fluid) at any instant of time. Furthermore, by calculating the total absorbency over the entire isosurface at each time step, the temporal rise or decay in secondary fluid concentration is determined. Insofar as the mass density of fluid is linearly proportional to the absorbency at a given x–value, the cell fractions computed along a given strip are converted to experimental absorbency values by plain normalization.

Results from the numerical simulations are shown in Fig. 3 at a Reynolds number of 60. Therein, the evolution of the tracer fluid in the downward direction is illustrated at several times. It should be noted that, for the same flow Reynolds number, an upward motion is accompanied by a blunter (i.e. flatter) profile. The comparatively increased elongation in downward flow can be attributed to the interplay between viscous and gravitational forces that act in opposite directions. The dominance of viscosity near the wall, where the mass of heavier fluid is smallest, gives rise to a relatively large local resistance to flow. Near the core, however, gravity dominates over viscosity, leading to an accelerated downward motion. This impression of opposing forces at both ends of the fluid-fluid interface causes a stretching of the tracer fluid. Besides the elongated shape seen in Fig. 3, a relatively smaller velocity gradient and, thereby, shear stress are produced at the wall.

When the flow is upward, a converse behavior is observed. In this case, the forces due to viscosity (near the wall) and gravity (near the core) are both acting downwardly. Their relative influence in the downward direction remains of the same order across the radius of the tube, thus leading to a more uniform interface between primary and secondary fluids. The ensuing profile is accompanied by more pronounced shearing rates near the wall where the velocity gradient is steepened by necessity.

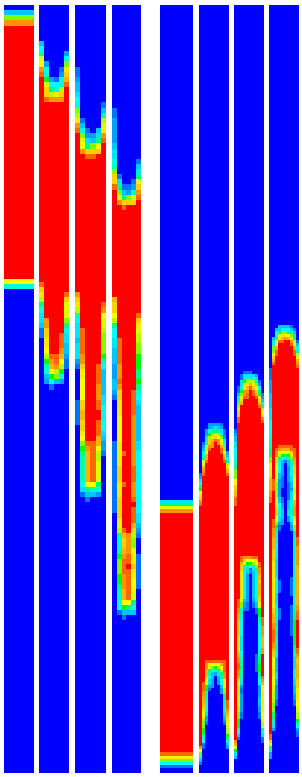

Fig. 3 Downward and upward flow-development of the secondary tracer fluid in a vertical tube at the same Reynolds number of 60.

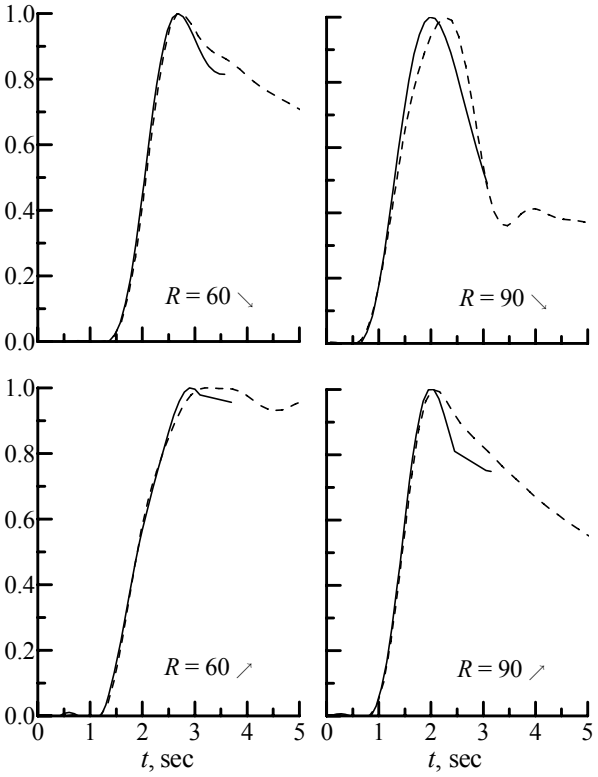

Fig. 4 Numerical (——) and experimental (- - -) absorbency time traces for two Reynolds numbers corresponding to either downward or upward flow.

Figure 3 illustrates the possibility of capturing the essential flow characteristics throughout the tube. In order to draw comparisons with experimental results, attention must be shifted to the fraction of tracer fluid at the x-ray measurement site. Along that isosurface, the total absorbency is calculated by summing the fractions of secondary fluid along that cross-section. As shown in Fig. 4, these results can be generated and plotted alongside the experimentally acquired samples. In all four cases, results converge in predicting a faster decay of tracer fluid concentration at higher Reynolds number. For the same Reynolds number, the steeper decay of tracer fluid occurs in the downward pass due to the more noticeable elongation of tracer fluid throughout the tube.

Rather than focus on the total absorbency at a given cross section, Fig. 5 displays the temporal cross-sectional concentrations of tracer fluid. These are shown for the same four cases of Fig. 4 using both experimental and numerical simulations. Although there is considerable

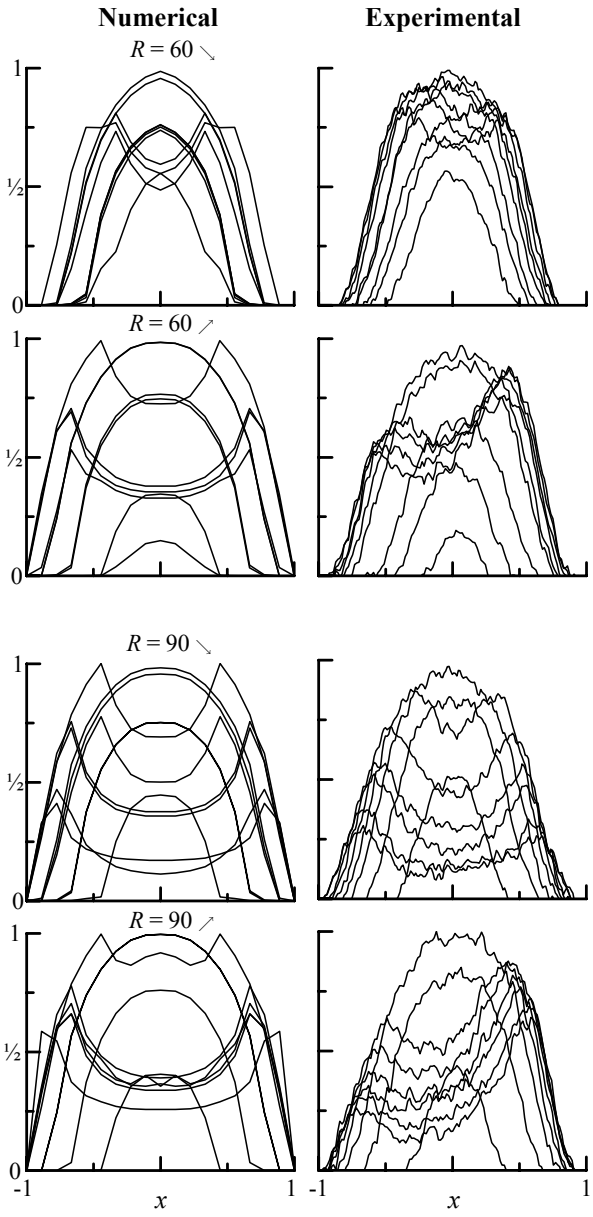

Fig. 5 Numerical and experimental absorbency profiles for two Reynolds numbers corresponding to either downward or upward flow. Each inset displays 9 curves separated by a fixed time step of 0.1 and 0.15 seconds for the low and high Reynolds numbers, respectively.

asymmetry in the experimental data, agreement with trend in the numerical simulations can be observed. The asymmetry is apparently due to imperfection in the tracer form during injection.

At the low Reynolds number of 60, it can be seen in the top half of Fig. 5 that the downward flow exhibits narrower bell-shaped concentration curves near the tracer front than those obtained

during the upward flow. This observation is corroborated by adjacent experimental samples and supports the hypothesis made earlier regarding the gravity-induced stretching of the tracer fluid during the downward pass.

At the higher Reynolds number of 90, the bottom half of Fig. 5 displays a smaller difference between upward and downward flows. This may be attributed to the weaker role played by gravity at higher Reynolds numbers.

5 CONCLUSIONS

In this study, a numerical simulation is presented as a tool for investigating the two-phase flow development of a tracer fluid having a different density than the primary medium in which it is immersed. The numerical procedure developed here enables us to reproduce concentration profiles along the entire length of tubing. When applied to a vertical flow, the numerical solutions are able to mimic experimentally produced concentration profiles measured at a discrete spatial location. In the four sample cases described, laboratory and computational results converge in predicting the effect of gravity on the shape of the tracer fluid: In gravity-assisted motion, a stretching of the profile is detected. The elongation of the resulting tracer fluid becomes less appreciable at higher Reynolds numbers. In gravity-resisted motion, a blunter profile is obtained with steeper velocity gradients at the wall. Now that a viable methodology is in place, more work is required to cover a broader range of operating parameters, aspect ratios, and flow orientations. Additional issues that merit consideration include varying density ratios and characterizing the onset of flow breakup and instability.

ACKNOWLEDGMENTS

This work was sponsored by the Falk Grant, Medical College of Wisconsin, Milwaukee, WI. The authors are deeply grateful to Dr. Steven T. Haworth from the Zablocki V. A. Medical Center, Milwaukee, WI, for his assistance in acquiring the experimental measurements.

REFERENCES

[1] Clough, A. V., Haworth, S. T., Roerig, D. L., Hanger, C. C., and Dawson, C. A., 2001, "X-Ray Measurement of Regional Blood Flow Distribution Using Radiopaque Contrast Medium: Influence of Gravity," Proc. SPIE Internat. Soc. Optical Engrg, 4321, pp. 298-304.

[2] Freeney, P., and Marks, W., 1986, "Hepatic Perfusion Abnormalities During Ct Angiography: Detection and Interpretation," Radiol., 159, pp. 685-691.

[3] Tarver, D. S., and Plant, G. R., 1995, "Case Report: The Effect of Contrast Density on Computed Tomographic Arterial Portography," Brit. J. Rad., 68, pp. 200-203.

[4] Clough, A. V., Haworth, S. T., Hanger, C. C., Wang, J., Roerig, D. L., Linehan, J. H., and Dawson, C. A., 1998, "Transit Time Dispersion in the Pulmonary Arterial Tree," J. Appl. Physiol., 85, pp. 565-574.

[5] White, F. M., Fluid Mechanics, 4th ed., McGraw Hill, 1999.

[6] Fluent Uns Theory Manual, 4.8 ed., Fluent Inc., Palo Alto, California, 1998.